International Journal of Aeronautical and Space Sciences (2022) 23:1043–1052
https://doi.org/10.1007/s42405-022-00486-z

IJASS International Journal of Aeronautical and Space Sciences

ORIGINAL PAPER

A Path Stretching Model for Effective Terminal Airspace Management

Ramazan Kursat Cecen[1]

Received: 20 October 2021 / Revised: 23 March 2022 / Accepted: 24 May 2022 / Published online: 27 June 2022

Abstract
This study presents a mathematical model to optimize the total fuel consumption per aircraft for the aircraft landing problem (ALP) using the path stretching (PS) method. The PS model applies vector maneuver (VM), speed reduction (SR), and flight path angle (FPA) change methods for aircraft operation. In addition, two different mixed-integer linear programming models utilizing the point merge system (PMS) are presented to compare the PS model as PMS is a widely used method in ALP. The first PMS model uses the VM to handle arrival traffic and solve aircraft conflicts. The second one implements the VM and the SR techniques. Furthermore, an exact solution algorithm is selected to obtain the optimal solution. The PS model aims to increase the number of continuous descent operations by eliminating the level flights. Two different linear regression equations are generated to calculate the fuel consumption and flight time values in descent operations considering realistic aircraft parameters, FPA, and average airspeed. The results demonstrate that the PS model can reduce the total fuel consumption per aircraft by 8.94% and 3.45% compared to the PMS models.

Keywords Aircraft landing problem · Mixed-integer linear programming · TMA management · Fuel consumption · Path stretching · The point merge system

1 Introduction

The demand for air transportation has been dramatically increasing, and prediction indicators show that this trend will continue in the future. Although Covid-19 harms air traffic operations, it should return to the 2019 level by 2026, as predicted by Eurocontrol [1]. In addition, Eurocontrol [2] indicated that the number of passengers from the European region will reach 2.05 billion by 2040. These increases cause congestion at the airport and airspace, especially in terminal maneuvering area (TMA). This situation also increases schedule delays, flight delays, fuel consumption, CO2 emissions, and noise problems due to holding points and level flights during the descent phase. TMA is a complex area having arrival-departure operations, holding points, single-multiple runway airports, metroplex airports. Thus, traffic management becomes a more critical and sophisticated process within busy TMAs. Sequencing and scheduling arrival aircraft are essential to enhance the efficiency of aircraft operations in terms of time, fuel, emission, and noise cost in the boundary of TMA and to increase the utilization of the capacity efficiently. The problems on sequencing and scheduling aircraft are called aircraft sequencing and scheduling problem (ASSP) in the literature. The presented study focuses on arrival traffic flow in TMA, and it is called aircraft landing problem (ALP) in the literature, which is the sub-problem of the ASSP. The ALP has been studied widely, and detailed literature reviews have been presented [3–5]. The exact solution approaches employed in the ALP are given as follows: CPLEX solver [6–11], dynamic programming [12–17], and branch and bound (B&B) algorithm [18–20] have been applied as exact solution algorithms. Samà et al. [5] presented a mixed-integer linear programming (MILP) model for the aircraft scheduling problem with different objective functions. The objectives were to minimize the delay, limit the number of delayed aircraft and maximize runway throughput. Bennell et al. [15] presented a multi-objective dynamic programming model that considers runway throughput, early or late for landing, and fuel consumption caused by airborne delay. Samà et al. [20] addressed a scheduling problem in TMA and solved this problem by employing an alternative graph formulation. They aimed to minimize the delays and travel times of aircraft. Beasley et al. [21] focused on

✉ Ramazan Kursat Cecen
ramazankursat.cecen@ogu.edu.tr

[1] Eskisehir Osmangazi University, Eskisehir, Turkey

arrival sequencing at London Heathrow to improve the runway utilization via a heuristic algorithm. Pohl et al. [22] proposed a time-discrete model for ASSP during winter operations. They integrated the column generation with constrained programming methods to reduce the cost of delay. They used Munich Airport data, and the result showed that their approach surpassed the continuous-time method. Cecen et al. [23] proposed a stochastic mathematical model for ASSP. They aimed to decrease total aircraft delay considering wind direction uncertainties. Prakash et al. [24] proposed a new data-splitting algorithm for aircraft sequencing problems using mixed-integer programming (MIP) approach. Their algorithm could solve random examples in a reasonable time duration. Ahmadian and Salehipour [25] studied ALP using a metaheuristic algorithm. They employed a relax and solve algorithm to solve this problem. They compared the metaheuristic algorithm with the CPLEX solver. The result demonstrated that the proposed metaheuristic could solve problems including 500 aircraft within sixty seconds. Saez et al. [26] presented a new approach for the arrival operations using a MIP model. They use dynamic route and speed assignments to increase the number of continuous descent operations (CDO). In addition, they aimed to minimize path length and tree weight together. Ng et al. [27] presented a robust ASSP model to reduce delay. They used the min–max regret approach and an effective bee colony algorithm to solve this problem. The results showed that the proposed algorithm could obtain feasible results within 5 min. Rodríguez-Díaz et al. [28] implemented the simulated annealing algorithm for the aircraft scheduling problem. They aimed to minimize delay within the reasonable computational time. The results demonstrated that the algorithm reduced the delays at Gatwick airport. Kaplan and Cetek [29] presented a mathematical model to sequence arrival operations, and they used the Clonal Selection Algorithm. The results showed that their algorithm could reduce the delay and serve four more aircraft per hour comparing the FCFS approach. Rodríguez-Díaz et al. [30] presented a bi-objective model to minimize fuel consumption, aircraft delay, and noise using the constrained position approach. They used actual data from Madrid-Barajas airport, and the model could reduce total fuel consumption by 4.5% without rising noise levels. Hammouri et al. [31] developed an algorithm combining iterated local search and simulated annealing algorithms. They aimed to obtain an aircraft sequencing considering a predefined arrival time frame. Faye [32] proposed a quadratic time algorithm to reveal landing times that minimize the overall cost, depending on the aircraft delay duration. Dahlberg et al. [33] presented a MIP model to determine arrival routes in a TMA and minimize flight routes from entry to touchdown. Their approach could give feasible merge trees, ensuring that all aircraft were separated. Pawelek et al. [34] assessed replacing current methods for aircraft sequencing and merging to enable CDO by providing accurate information for the remaining distance to the runway. Dalmau et al. [35] tried to combine the assignment of RTAs and fixed routes to handle traffic peaks by utilizing the trombone procedures in Frankfurt Airport. Sáez et al. [36] proposed a model to sequence traffic in TMA with 4D closed-loop instructions to provide CDO by considering fuel and time costs. They used the model in Berlin-Schonefeld airport. Sáez et al. [37] proposed an enhanced trombone system to maximize the CDO operations using idle thrust descent and no speed brake. Liang et al. [38] presented a multi-layer PM to sequence and merge arrival flows on two parallel runways with conflict-free solutions. Then, the study by Liang et al. [38] focused on integrating arrival-departure flows for Beijing Capita less than 5 min of International Airport by employing RHC and Simulated Annealing for long-distance trajectories operations. Cecen [39] presented an MLIP model to decrease fuel consumption for extended TMA operations using the point merge system (PMS) system. In this study, vector maneuver (VM) and speed reduction (SR) techniques were implemented. Saez and Prats [40] discussed the difference between powered descent operations, and path stretching (PS) approaches using an optimal control approach. They compared the fuel consumption of two approaches for a single aircraft.

This study presents a new MILP model based on the PS technique to solve ALP. The two MILP models of PMS are also used to compare the proposed model. The first PMS model uses VM and sequencing legs to handle arrival traffic. The second model (PSM-SR) also implements the SR, VM, and sequencing legs to regulate air traffic. They aim to minimize the total fuel consumption (TFC) per aircraft. The PS model uses the SR and VM methods. Unlike the PMS model, the PS model can provide different flight path angles (FPA) during descent operations with the SR method. The outputs of the three MILP models are compared regarding fuel consumption and total flight time (TFT). We aim to demonstrate the usefulness of the PS method for total fuel consumption and the ease of implementation for ATCos operations in this study. Also, in this study, aircraft use their assigned FPA angle during the descent operations. The contributions of this study are presented followings: First, the PS and PMS models are proposed and compared, including SR, VM, and FPA changes. In addition, their effects upon the TFC and TFT are considered. Second, the conventional PMS and PMS-SR models were compared with the PS model, and the fuel consumption relationship was given in detail. Lastly, the fuel consumption and flight time estimation during descent operations are obtained using linear regression equations via realistic aircraft parameters.

The remaining paper is structured as follows: Sect. 2 and 3 define the problem and introduce the mathematical models; Sects. 4 and 5 reveal the experimental results and conclusion.

2 Problem Definition

The practical and efficient sequencing of the aircraft in the TMA is essential for conflict-free arrival operations. The ALP problem is an optimization problem that aims to obtain an optimum or near optimum arrival sequence while optimizing the objective functions without violating the operational constraints. This problem can be applied to single or multi runway airports. Safe separation among the aircraft can be maintained using the VM and the SR instructions. These techniques also determine the runway use times for each aircraft, and all these techniques can be implemented simultaneously. This study concentrates on the arrival flights in Istanbul Sabiha Gökçen International Airport (LTFJ).

This study assumes that TMA uses seven entry points, two merging points (MPs), and a final approach point (FAP) for the PS model presented in Fig. 1. The distance of each entry point to the merge point is the same. The MPs are located at the transition altitude. Therefore, each aircraft can perform SR and FPA change techniques from entry to merge points. After crossing the transition altitude, each aircraft follows the BADA 3.11 [41] descent profile with defined airspeed and FPA. The fuel consumption values from transition altitude to landing were used according to the BADA 3.11. Similarly, the PMS model also uses seven entry points, two vertically separated sequencing legs, the lower at transition altitude, and a merge point shown in Fig. 2.

One type of aircraft, which is medium, was selected for this study. The vortex separations are given in Table 1 to maintain safe arrival (A) operations.

Each arrival flight is directed to one merge point regarding its entry point. Aircraft conflict situations are controlled on the two merge points and the runway. As the proposed model minimizes TFC per aircraft, we obtained a linear regression equation for fuel consumption, and descent time estimations were obtained using BADA 3.11 parameters. To calculate the fuel consumption during descent operations, it is required to calculate the following essential value according to BADA

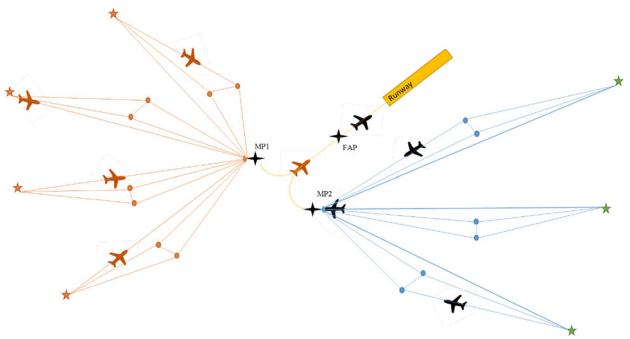

Fig. 1 TMA route structure for PS model

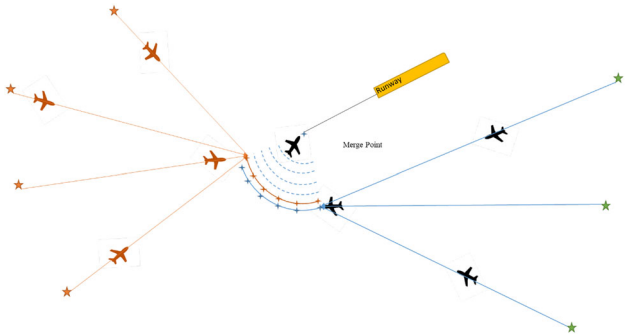

Fig. 2 TMA route structure for PMS models

Table 1 Vortex separations, in seconds (Cecen et al. [23])

Leading–trailing aircraft	Operation type A–A
Medium–medium	72

3.11: maximum climb thrust ($\mathrm{Thr}_{\mathrm{max,climb}}$), which depends on

- $C_{\mathrm{Tc},1}$, $C_{\mathrm{Tc},2}$, $C_{\mathrm{Tc},3}$ are climb thrust coefficient.
- $C_{\mathrm{Tc},4}$, $C_{\mathrm{Tc},5}$ are thrust temperature coefficient.
- Geopotential pressure altitude (H_p) (feet).
- Temperature deviation from the standard atmosphere (ΔT).

$$\left(\mathrm{Thr}_{\mathrm{max,climb}}\right)_{\mathrm{ISA}} = C_{\mathrm{Tc},1}\left(1 - \frac{H_{\mathrm{p}}}{C_{\mathrm{Tc},2}} + C_{\mathrm{Tc},3}H_{\mathrm{p}}^2\right), \quad (1)$$

$$\left(\mathrm{Thr}_{\mathrm{max,climb}}\right) = \left(\mathrm{Thr}_{\mathrm{max,climb}}\right)_{\mathrm{ISA}}\left(1 - C_{\mathrm{Tc},5}\cdot\Delta T_{\mathrm{eff}}\right), \quad (2)$$

where ΔT_{eff} is calculated via Eq. (3):

$$\Delta T_{\mathrm{eff}} = \Delta T - C_{\mathrm{Tc},4}. \quad (3)$$

The necessary descent thrust is calculated using the ratio of $\mathrm{Thr}_{\mathrm{max,climb}}$ using different flight configurations: descent operations higher than transition altitude $\left(C_{\mathrm{Tdes,high}}\right)$, descent operations lower than transition altitude $\left(C_{\mathrm{Tdes,low}}\right)$, approach $\left(C_{\mathrm{Tdes,app}}\right)$, and landing $\left(C_{\mathrm{Tdes,ld}}\right)$.

$$\mathrm{Thr}_{\mathrm{des,high}} = C_{\mathrm{Tdes,high}}\cdot\mathrm{Thr}_{\mathrm{max,climb}}, \quad (4)$$

$$\mathrm{Thr}_{\mathrm{des,low}} = C_{\mathrm{Tdes,low}}\cdot\mathrm{Thr}_{\mathrm{max,climb}}, \quad (5)$$

$$\mathrm{Thr}_{\mathrm{des,app}} = C_{\mathrm{Tdes,app}}\cdot\mathrm{Thr}_{\mathrm{max,climb}}, \quad (6)$$

$$\mathrm{Thr}_{\mathrm{des,ld}} = C_{\mathrm{Tdes,ld}}\cdot\mathrm{Thr}_{\mathrm{max,climb}}. \quad (7)$$

The minimum fuel flow (f_{min}, kg/min) higher than transition altitude is calculated using the following equation:

$$f_{\text{min}} = C_{\text{f3}}\left(1 - \frac{H_{\text{p}}}{C_{\text{f4}}}\right), \tag{8}$$

where using aircraft-specific coefficients (C_{f1}, C_{f2}, C_{f3}, C_{f4}). The nominal fuel consumption (f_{nom}) is estimated using the true airspeed (V_{TAS}), thrust specific fuel consumption (η) and thrust (Thr) values.

$$\eta = \left(C_{\text{f1}}\left(1 + \frac{V_{\text{TAS}}}{C_{\text{f2}}}\right)\right), \tag{9}$$

$$f_{\text{nom}} = \text{Thr} \cdot \eta. \tag{10}$$

The fuel consumption during the approach f_{app} and landing f_{ld} phases are estimated and given in the following equations:

$$f_{\text{app/ld}} = \text{MAX}(f_{\text{nom}},\ f_{\text{min}}). \tag{11}$$

While aircraft descending from the top of the descent point to transition altitude generally use idle engine configurations, Eq. (8) should be used to calculate fuel consumption. As it is shown in Eq. (8), the fuel consumption is directly affected by aircraft altitude H_{p} and aircraft-specific coefficients (i.e.,C_{f1}, C_{f2}). Also, the unit of f_{min} is kg/min, hence it is also directly affected by the rate of descent (ROD) value. ROD can be calculated using aircraft FPA and aircraft airspeed. These values can also change the fuel consumption and flight time as it lengthens or shortens flight paths. In this study, each ROD value from the altitude of the top of the descent point to transition altitude for each consecutive flight level is calculated. Then, each descending fuel consumption value and flight duration between two subsequent flight levels are determined. With FPA and average airspeed values, two linear regression equations for fuel consumption and flight time are obtained. As the equations are demonstrated, linear regression Eqs. (12)–(13) are obtained, and the relationship between the fuel consumption (kg) and average airspeed (v_i) (knot) and FPA (fpa_i) (°) is given in Fig. 3.

$$u_{00} + u_{10} \cdot \text{fpa}_i + u_{01} \cdot v_i, \tag{12}$$

$$p_{00} + p_{10} \cdot \text{fpa}_i + p_{01} \cdot v_i, \tag{13}$$

where u_{00}, The constant value in the regression equation, u_{10}, the coefficient value of FPA, u_{01}, The coefficient value of average airspeed in the regression equation for fuel consumption. Similarly, the relationship of flight duration with average airspeed (v_i) and FPA $\left(\text{fpa}_i\right)$ is given in Fig. 4. The

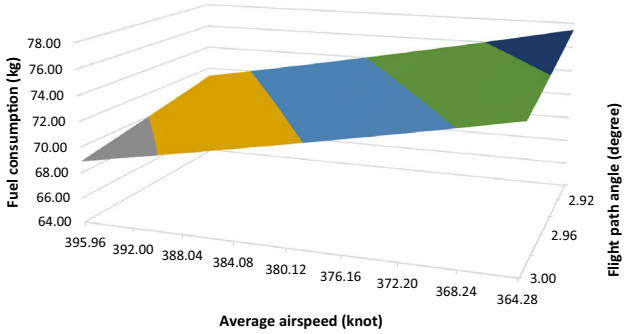

Fig. 3 The fuel consumption changes regarding the average airspeed and FPA

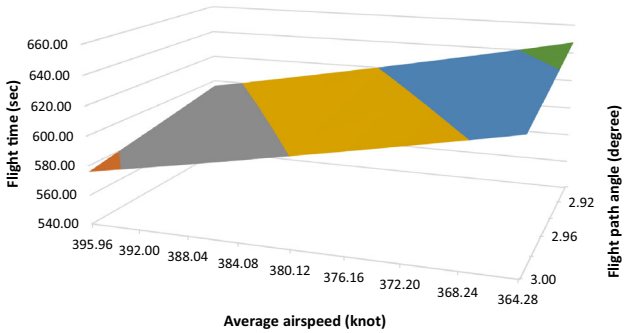

Fig. 4 The flight time changes regarding the average airspeed and FPA

adjusted R^2 values were estimated as 0.99 for both the fuel consumption and flight time equations.

Where p_{00}, The constant value in the regression equation, p_{10}, the coefficient value of FPA, p_{01}, The coefficient value of average airspeed in the regression equation for flight time estimation. The flight time and fuel consumption values represent the altitude between the top of descent and transition altitude. Each flight level airspeed is selected using BADA 3.11 values, and the SR method is applied using these values. The aircraft airspeed during the descending operation is limited between 250 calibrated airspeed (CAS) and 300 CAS. V_{nom} is the average airspeed value between the top of descent and transition altitude. Average airspeed is calculated using each flight level airspeed value. The SR approach considers these minimum and maximum values. The nominal FPA is assumed as 3° and the variation in the FPA is permitted to be between 3° and 2.9°. Besides, the SR technique is implemented between V_{nom} and $0.92V_{\text{nom}}$ values.

3 Mathematical Models

The PS method uses a different arrival route structure to maintain safe separation while supporting CDO. Also, this method is implemented with the SR method in this study. In addition, the PMS is a sequencing approach that permits aircraft to

use area navigation (R-NAV) routing. The PMS consists of two parallel sequencing legs and a merge point. This method includes level flight during the flights on the sequencing legs, and aircraft perform a level flight "until direct to a merge point" to instruction. This approach maintains CDO before entering sequencing legs and after directing instruction. The objective functions of both PS and PMS approaches are to minimize the fuel consumption per aircraft. The mathematical models are given sub-sections for the ALP.

3.1 The Mathematical Model of the PS Approach

Indices
I set of aircraft in the sector i, i_1,$i_2 \in I$.
Parameters
T: Radar separation in seconds.
S: Vortex separation in seconds.
M: large enough positive number

$$M = \left(\left(\mathrm{et}_{i_2}\right) - \left(\mathrm{et}_{i_1}\right)\right) \cdot 2,$$

where i_1 and i_2 are the first and the last aircraft entering the TMA, respectively.
an: number of aircraft.
et_i: entry time of TMA for aircraft i.
mp_i: approach side of aircraft i.
R: flight duration from the merge point to the runway.
p_{00}: constant value in the regression equation.
p_{10}: coefficient value of FPA in the regression equation.
p_{01}: coefficient value of average airspeed in the regression equation.
u_{00}: constant value in the regression equation for fuel consumption.
u_{10}: coefficient value of FPA in the regression equation for fuel consumption.
u_{01}: coefficient value of average airspeed in the regression equation for fuel consumption.
u: cost of delay time per second before entering the TMA.
dc: total fuel consumption of descending from transition altitude to the runway.
V_{nom}: nominal average airspeed of aircraft during descent operations from the entry of TMA to merge points according to BADA 3.11 values.
Decision Variables
mt_i: crossing time of the assigned merge point of aircraft i.
t_i: arrival time of aircraft i.
d_i: delay time of aircraft i before entering the TMA.
v_i: average airspeed of aircraft i.
fpa_i: gliding angle of aircraft i.
tf_i: flight duration of aircraft i.
y_{i_1,i_2}: 0–1 variable that takes a value of 1 if aircraft i_1 uses the runway before aircraft i_2; otherwise, it is zero.

The constraints and objective function used in the mathematical model are as follow:

Constraint (14) calculates the arrival time of two merge points using the entry time of TMA, delay duration before TMA entrance, and descent time from TMA entrance to the merge point.

$$\mathrm{mt}_i = \mathrm{et}_i + d_i + p_{00} + p_{10} \cdot \mathrm{fpa}_i + p_{01} \cdot v_i \forall i, \tag{14}$$

Moreover, Constraint (15) and (16) control the radar separation for the merge points if the aircraft i_1 and aircraft i_2 use the merge point in their descent operations.

$$\mathrm{mt}_{i_2} - \mathrm{mt}_{i_1} \geq T - \left(1 - y_{i_1,i_2}\right)M \quad \forall i_1,\, i_2 | i_1 \neq i_2,\, \mathrm{mp}_{i_1} = \mathrm{mp}_{i_2}, \tag{15}$$

$$\mathrm{mt}_{i_1} - \mathrm{mt}_{i_2} \geq T - \left(y_{i_1,i_2}\right)M \quad \forall i_1,\, i_2 | i_1 \neq i_2,\, \mathrm{mp}_{i_1} = \mathrm{mp}_{i_2}. \tag{16}$$

Constraint (18) calculates the arrival time of each aircraft.

$$t_i = \mathrm{mt}_i + R \forall i. \tag{17}$$

In addition, Constraint (18) and (19) check the vortex separation for the final approach point.

$$t_{i_2} - t_{i_1} \geq S - \left(1 - y_{i_1,i_2}\right)M \quad \forall i_1,\, i_2 | i_1 \neq i_2, \tag{18}$$

$$t_{i_1} - t_{i_2} \geq S - \left(y_{i_1,i_2}\right)M \quad \forall i_1,\, i_2 | i_1 \neq i_2. \tag{19}$$

Constraint (20) calculates the flight duration for each aircraft.

$$\mathrm{tf}_i = t_i - \mathrm{et}_i \quad \forall i. \tag{20}$$

Constraint (21) and (22) limit the SR and FPA change during descent operations.

$$0.92 \cdot V_{\mathrm{nom}} \leq v_i \leq V_{\mathrm{nom}}, \tag{21}$$

$$2.9^\circ \leq \mathrm{fpa}_i \leq 3^\circ. \tag{22}$$

Objective (23) calculates the fuel consumption per aircraft.

$$\sum_i \frac{(d_i \cdot u)}{\mathrm{an}} + \sum_i \frac{\left(u_{00} + u_{10} \cdot \mathrm{fpa}_i + u_{01} \cdot v_i\right)}{\mathrm{an}} + \mathrm{dc}. \tag{23}$$

Constraints (24–28) are sign constraints.

$$\mathrm{fpa}_i,\, \mathrm{mt}_i \geq 0 \quad \forall i \in I, \tag{24}$$

$$\mathrm{tf}_i,\, d_i \geq 0 \quad \forall i \in I, \tag{25}$$

$$t_i,\ v_i \geq 0 \quad \forall i \in I, \tag{26}$$

$$y_{i_1,i_2} \in \{0,\ 1\} \quad \forall i_1,\ i_2 \in I. \tag{27}$$

3.2 The Mathematical Models of the PMS Approach

Two different PMS models were used in this subsection. The first PMS model uses sequencing legs and VM methods to regulate air traffic and includes the Eqs. (29), (31)–(37), and (39)–(43). The second PMS model applies the VM and the SR containing the Eqs. (30)–(43).

Indices

I set of aircraft in the sector i, i_1,$i_2 \in I$.

K set of turn points $k \in K$.

Parameters

T: Radar separation in seconds.

S: Vortex separation in seconds.

M: Large enough positive number

$$M = \left(\left(\mathrm{et}_{i_2}\right) - \left(\mathrm{et}_{i_1}\right)\right) \cdot 2,$$

where i_1 and i_2 are the first and the last aircraft entering the TMA, respectively.

An: number of aircraft.

et_i: entry time of TMA for aircraft I.

mp_i: approach side of aircraft I.

E: average flight duration from the sequencing legs to the runway.

O: distance from the entry point to sequencing legs.

$V2$: airspeed of aircraft during the sequencing leg.

dc: total fuel consumption value from the sequencing legs to the runway.

u: cost of delay time per second before entering the TMA.

$u1$: average cost of descending up to sequencing legs.

$u2$: cost of airspeed traveling on the sequencing legs per second.

v_i: average airspeed of aircraft i.

V_{nom}: nominal average airspeed of aircraft during descent operations from the entry of TMA to merge points according to BADA 3.11 values.

Decision Variables

$c_{i,k}$: 0–1 variable that takes a value of 1 if aircraft i uses the turning point of k; otherwise, it is zero.

vsr_i: average airspeed of aircraft i.

t_i: arrival time of aircraft i.

tf_i: flight duration of aircraft i.

d_i: delay time of aircraft i before entering the TMA.

st_i: entering time of sequencing leg for aircraft i.

y_{i_1,i_2}: 0–1 variable that takes a value of 1 if aircraft i_1 uses the runway before aircraft i_2; otherwise, it is zero.

The constraints and objective function used in the mathematical model are as follow:

Constraint (29) and (30) calculate both the arrival time of sequencing legs using the entry time of TMA, delay duration before TMA entrance, and descent time from TMA entrance to sequencing legs. However, Constraint (30) allows each aircraft to determine its average descend airspeed.

$$\mathrm{st}_i = \mathrm{et}_i + d_i + \frac{O}{v_i} \quad \forall i, \tag{28}$$

$$\mathrm{st}_i = \mathrm{et}_i + d_i + \frac{O}{\mathrm{vsr_i}} \quad \forall i, \tag{29}$$

Furthermore, Constraint (31) and (32) control the aircraft separation for sequencing legs if the aircraft i_1 and aircraft i_2 use the sequencing legs.

$$\mathrm{st}_{i_2} - \mathrm{st}_{i_1} \geq T - \left(1 - y_{i_1,i_2}\right)M \quad \forall i_1,\ i_2 | i_1 \neq i_2,\ \mathrm{mp}_{i_1} = \mathrm{mp}_{i_2}. \tag{30}$$

$$\mathrm{st}_{i_1} - \mathrm{st}_{i_2} \geq T - \left(y_{i_1,i_2}\right)M \quad \forall i_1,\ i_2 | i_1 \neq i_2,\ \mathrm{mp}_{i_1} = \mathrm{mp}_{i_2}. \tag{31}$$

Constraint (33) calculates whether an aircraft uses a turning point on the sequencing legs or not.

$$\sum_k c_{i,k} \leq 1. \tag{32}$$

Constraint (34) calculates each aircraft's arrival time, calculating the travel duration on the sequencing legs and flight durations between the sequencing leg and the final approach point.

$$t_i = \mathrm{st}_i + \frac{\left(\sum_k c_{i,k} \cdot k\right)}{V2} + E. \tag{33}$$

In addition, Constraint (35) and (36) control the vortex separation for the runway for each aircraft pair.

$$t_{i_2} - t_{i_1} \geq S - \left(1 - y_{i_1,i_2}\right)M \quad \forall i_1,\ i_2 | i_1 \neq i_2, \tag{34}$$

$$t_{i_1} - t_{i_2} \geq S - \left(y_{i_1,i_2}\right)M \quad \forall i_1,\ i_2 | i_1 \neq i_2. \tag{35}$$

Constraint (36) calculates the flight duration for each aircraft.

$$\mathrm{tf}_i = t_i - \mathrm{et}_i \quad \forall i. \tag{36}$$

Constraint (37) limits the airspeed value for the aircraft set.

$$0.92 \cdot V_{\mathrm{nom}} \leq \mathrm{vsr}_i \leq V_{\mathrm{nom}}. \tag{37}$$

Table 2 Outputs of the models

Scenario	PS FC	PMS FC	PMS-SR FC	PS FT	PMS FT	PMS-SR FT	PS CPU	PMS CPU	PMS-SR CPU
1	245.91	267.57	252.78	881.27	886.27	881.27	0.13	0.46	0.4
2	248.33	265.64	252.93	879.17	884.17	879.17	0.18	0.24	0.24
3	257.79	288.05	268.92	908.96	913.84	908.84	0.65	4.81	1.14
4	277.16	306.07	289.31	932.24	937.24	932.24	4.49	17.69	14.33
5	245.92	268.28	254.12	881.78	886.78	881.78	0.18	0.46	0.32
6	246.90	261.89	251.28	873.48	877.88	872.88	0.11	0.25	0.16
7	255.62	292.88	271.36	914.84	919.64	914.64	0.48	19.51	6.24
8	250.68	282.60	263.14	900.94	905.94	900.94	0.23	3.74	0.9
9	258.49	293.83	274.16	916.20	920.72	915.84	0.67	22.62	7.04
10	267.46	299.12	282.35	922.25	927.25	922.25	5.90	43.28	22.65
11	247.85	271.06	254.98	886.09	889.68	885.52	0.16	0.77	0.33
12	247.71	270.99	255.51	885.44	890.42	885.42	0.26	0.58	0.32
13	256.28	290.53	271.46	912.05	917.05	912.17	1.13	14.88	6.6
14	256.54	286.62	266.03	907.12	912.10	907.24	0.65	3.49	0.72
15	245.87	267.28	252.46	881.04	885.68	881.16	0.11	0.39	0.43
16	244.07	256.39	246.69	864.83	869.47	864.65	0.14	0.31	0.22
17	246.26	268.72	254.01	882.23	886.74	881.75	0.23	0.39	0.48
18	258.34	286.45	269.72	906.21	911.09	906.21	0.85	4.71	1.28
19	244.16	257.07	247	866.95	871.41	866.9	0.23	0.12	0.18
20	245.11	261.10	249.83	872.33	876.97	872.21	0.21	0.21	0.17
Average	252.32	277.11	261.40	893.77	898.52	893.65	0.85	6.95	3.21

Objective (38) calculates the fuel consumption per aircraft for descent operations, including the fuel consumption right before TMA due to delay, descent operations, traveling along the sequencing legs, and descending to the runway.

$$\sum_i \frac{d_i \cdot u}{\text{an}} + \sum_i \frac{u1}{\text{an}} + \sum_i \frac{\left(\sum_k c_{i,k} \cdot k\right)}{V2} \cdot u2 + \text{dc}. \tag{38}$$

Constraints (38–41) are sign constraints.

$$\text{st}_i,\ t_i \geq 0 \quad \forall i \in I, \tag{39}$$

$$d_i,\ \text{vsr}_i \geq 0 \quad \forall i \in I, \tag{40}$$

$$c_{i,k} \in \{0,\ 1\}\ \forall i \in I \forall k \in K, \tag{41}$$

$$y_{i_1,i_2} \in \{0,\ 1\} \quad \forall i_1,\ i_2 \in I. \tag{42}$$

4 Computational Results

This section compared the three mathematical models to demonstrate the fuel consumption values among different TMA sequencing techniques. Moreover, detailed analyses were made for the approaches regarding the flight time, the number of aircraft used the SR, the number of aircraft used sequencing legs used, the number of aircraft used different FPA. The MILP models were implemented in GAMS/CPLEX solver. Twenty independent test problems were generated, and each one had a different traffic situation. For example, this airport can serve 40 aircraft during peak hours per hour [42]. Therefore, the scenarios use 20 aircraft per 30 min to represent a realistic traffic situation. In addition, exponential distribution was used to obtain TMA entrance time for each aircraft, and the uniform distribution was used to produce route information. The results are given in Tables 2 and 3. In Table 2, the first column shows the scenario number, from column 2 to column 4 shows the average fuel consumption per aircraft (FC) (kg) for PS, PMS, and PMS-SR models. The column from 5 to column 7 display the average flight time per aircraft (FT) (s). The column from 8 to column 10 demonstrate CPU time (s) for each model.

Table 3 Detail analysis of the models

Scenario	PS	PMS	PMS-SR	PS	PMS	PMS-SR	PS	PMS	PMS-SR	PS	PSM-SR	PS	PMS	PSM-SR
	FC max	FC max	FC max	FT max	FT max	FT max	NVM	NVM	NVM	NSR	NSR	NAC	NSL	NSL
1	256.45	318.87	288.22	955.92	950.92	950.92	2	12	5	12	12	6	10	8
2	303.97	390.92	335.74	1017.62	1044.49	1012.62	2	13	5	13	13	4	11	5
3	340.96	472.4	411.94	1065.66	1150.3	1111.59	5	15	8	15	15	8	14	10
4	415.98	462.37	483.06	1163.09	1137.28	1203.95	7	13	9	13	13	8	14	9
5	259.27	366.64	291.04	959.58	1012.96	954.58	1	11	7	11	11	8	9	8
6	297.86	360.28	329.63	1009.69	1004.69	1004.69	1	9	3	9	9	3	9	5
7	302.32	415.57	365.59	1015.49	1076.5	1051.39	7	15	8	16	16	12	12	13
8	299.44	361.86	331.21	1011.74	1006.74	1006.74	4	14	7	14	14	10	10	12
9	321.71	454.08	353.48	1040.67	1126.51	1035.67	8	15	8	15	15	11	14	11
10	427.20	490.59	458.97	1177.66	1173.92	1172.66	8	13	6	13	13	10	10	10
11	289.94	413.77	325.43	999.41	1074.17	999.23	2	11	5	12	12	5	13	7
12	286.58	381.32	318.35	995.04	1032.02	990.04	2	12	6	13	13	6	10	9
13	341.09	421.7	391.05	1065.83	1084.45	1084.45	6	15	9	15	15	10	13	11
14	373.94	425.13	405.73	1108.5	1088.91	1103.52	4	15	9	15	15	9	14	10
15	263.72	326.14	295.49	965.35	960.35	960.35	1	13	6	13	13	5	11	9
16	250.44	320.08	281.22	941.67	947.00	939.08	0	11	1	11	12	3	5	3
17	268.58	335.31	300.35	971.67	966.78	966.67	1	13	5	13	13	7	9	9
18	351.79	420.25	383.56	1079.74	1082.58	1074.74	6	13	9	13	13	8	12	11
19	247.61	292.93	262.69	917.93	916.52	917.76	0	8	4	9	9	4	8	5
20	261.15	323.56	294.77	962.01	957.01	959.42	1	10	4	10	10	4	9	6
Average	308.00	387.69	345.38	1021.21	1039.71	1025.01	3.40	12.55	6.2	12.75	12.8	7.05	10.85	8.55

The results show that the PS model reduced fuel consumption by 8.94% and 3.47% compared to PMS and PMS-SR approaches, respectively. Also, the PS model decreased the flight time by approximately 0.53% comparing the PMS approach, yet no decrease was estimated for the PMS-SR model. The reduction rates in flight time were not as noticeable as in fuel consumption for the PS model compared to PMS and PMS-SR models. The standard deviations of fuel consumptions were estimated as 8.45, 14.52, and 11.83 for PS, PMS, and PMS-SR models, respectively. In addition, the maximum difference of fuel consumption value among the scenarios was calculated at 33.09 kg. for scenarios 4 and 16 of the PS model. However, the maximum difference in fuel consumption value among the scenarios was estimated at 49.68 and 42.62 kg for the PMS and the PMS-SR, respectively. There are two main reasons for fuel consumption reduction. The first reason is that the aircraft performed level flight at 10,000 feet for both PMS and PMS-SR models for separation and sequencing maneuvers. Level flight is conducted with no FPA; therefore, fuel consumption increases. Similarly, the other reason is that the aircraft can perform a level flight to provide the necessary delay to avoid collisions before starting the descent movement. In addition, the average CPU times of the PS model were less than 1 s and the maximum CPU times were less than 6 s. However, the average CPU times of the PMS and the PMS-SR models were less than 7 and 3.5 s and the maximum CPU times were less than 44 s. And 32 s. In Table 3, the first column demonstrates the scenario number, the columns between 2 and 3 display the maximum and fuel consumptions for an aircraft in each scenario for PS and PMS, respectively. Also, columns 4 and 5 show the maximum flight time, the columns 6 and 7 demonstrate the number of VM, the SR, FPA, and point merge use. In Table 3, column 1 displays the scenario number. Columns 2 and 4 show the maximum fuel consumption (FC max) (kg) values for all models. Similarly, column 5 and column 7 display the maximum flight time (FT max) (s) values. Columns 8 and 10 present the number of aircraft that used VM (NVM) (count). Columns 11 and 12 show the number of aircraft that used the SR (NSR) (count). Column 13 displays the number of aircraft that changed FPA (NAC) (count). Columns 14 and 15 show the number of aircraft that used sequencing legs for PMS and PMS-SR models (NSL) (count).

The average maximum fuel consumptions were determined as 308 kg, 387.69, and 345.38 kg for the PS, PSM, and PMS-SR approaches. The maximum fuel consumption enhancement rate increased by 20.55% and %11.82. Also, the maximum flight times were determined as 1021.21, 1039.71, and 1025 s for the PS, PMS, and PMS-SR. The standard deviations were estimated to be 51.58, 56.42, and 59.1 for PS, PMS-SR models. While 68 aircraft use the VM for the PS model, 251 aircraft utilize the VM for the PMS model. Nonetheless, 124 aircraft used VM for the PMS-SR model among all scenarios. Furthermore, these results occurred because aircraft can only use sequencing legs and VM for the PMS model to maintain necessary delay. However, the PMS model can use VM and SR methods to avoid collisions. Therefore, the SR method affects fuel consumption considerably compared to non-SR methods. Furthermore, approximately 64% of aircraft SR for PS and PMS-SR models. In addition, 35% of aircraft utilized FPA change apart from 3° for the PS model. Also, 54.25% and 42.75% of aircraft used sequencing legs for PMS and PMS-SR models.

5 Conclusions

The study presents three different MILP models for ALP to minimize the average fuel consumption per aircraft within the TMA operations. While The first model used the PS method, the second and third models applied the PMS to obtain optimum aircraft sequencing. The proposed PS model provides the SR up to 8% of the nominal airspeed within the TMA. The descent fuel consumption up to transition point was estimated using a linear regression equation obtained by a realistic aircraft parameter using BADA 3.11. This equation calculates aircraft fuel consumption using average airspeed and FPA values. The models were compared to show which model provided better fuel optimum descent operations within the TMA. The results demonstrated that the PS model reduced the total fuel consumption by 8.94% and %3.45 comparing the PSM and PMS-SR models. Also, according to the results, the number of VM was applied in PMS more than PS and PMS-SR because the PMS approach needs to solve aircraft conflicts by only using VM, yet PS can use VM, SR, and change of FPA and PMS-SR can use VM, SR sequencing legs. While the number of aircraft that performed VM is slightly higher than the NSL for the PMS model, this situation has been swapped for the PMS-SR model since SR reduces the need for VM. The number of aircraft that need to be separated before entering the sequencing legs is high for the PMS model. However, the number of aircraft that performed NVM is noticeably lower than the NSL for the PMS model. The results showed that SR could considerably decrease VM demand for the TMA operations. This stochastic version can be investigated in the future, and extended TMA operations can be added to the models.

References

1. Eurocontrol (2020) Five-Year Forecast 2020–2024 European Flight Movements and Service Units: Three Scenarios for Recovery from COVID-19 (Issue November)
2. Eurocontrol (2018) European Aviation In 2040 Annex1 Flight Forecast to 2040
3. Dönmez K, Çetek C, Kaya O (2021) Aircraft sequencing and scheduling in parallel-point merge systems for multiple parallel runways. Transp Res Rec 2021:03611981211049410
4. Ikli S, Mancel C, Mongeau M, Olive X, Rachelson E (2021) The aircraft runway scheduling problem: a survey. Comput Oper Res 132:105336
5. Sama M, D'Ariano A, D'Ariano P, Pacciarelli D (2017) Scheduling models for optimal aircraft traffic control at busy airports: tardiness, priorities, equity and violations considerations. Omega 67:81–98
6. Vadlamani S, Hosseini S (2014) A novel heuristic approach for solving aircraft landing problem with single runway. J Air Transp Manag 40:144–148
7. Sama M, D'Ariano A, D'Ariano P, Pacciarelli D (2014) Optimal aircraft scheduling and routing at a terminal control area during disturbances. Transport Res Part C Emerg Technol 47:61–85
8. Lee S, Hong Y, Kim Y (2020) Optimal scheduling algorithm in point merge system including holding pattern based on mixed-integer linear programming. Proc Inst Mech Eng Part G J Aerosp Eng 234(10):1638–1647
9. Samà M, D'Ariano A, Palagachev K, Gerdts M (2019) Integration methods for aircraft scheduling and trajectory optimization at a busy terminal manoeuvering area. OR Spectr 41(3):641–681
10. Cecen RK, Çetek FA (2020) Optimising aircraft arrivals in terminal airspace by mixed integer linear programming model. Aeronaut J 124(1278):1129–1145
11. Cecen RK (2021) Multi-objective TMA management optimization using the point merge system. Aircr Eng Aerosp Technol 93(1):15–24
12. Balakrishnan H, Chandran BG (2010) Algorithms for scheduling runway operations under constrained position shifting. Oper Res 58(6):1650–1665
13. Boysen N, Fliedner M (2011) Scheduling aircraft landings to balance workload of ground staff. Comput Ind Eng 60(2):206–217
14. Lieder A, Briskorn D, Stolletz R (2015) A dynamic programming approach for the aircraft landing problem with aircraft classes. Eur J Oper Res 243(1):61–69
15. Bennell JA, Mesgarpour M, Potts CN (2017) Dynamic scheduling of aircraft landings. Eur J Oper Res 258(1):315–327
16. Montoya J, Rathinam S, Wood Z (2013) Multi-objective departure runway scheduling using dynamic programming. IEEE Trans Intell Transp Syst 15(1):399–413
17. Rathinam S, Wood Z, Sridhar B, Jung Y (2009) A generalized dynamic programming approach for a departure scheduling problem. In: AIAA guidance, navigation, and control conference, p 6250
18. D'Ariano A, Pistelli M, Pacciarelli D (2012) Aircraft retiming and rerouting in vicinity of airports. IET Intell Transport Syst 6(4):433–443
19. Sölveling G, Clarke JP (2014) Scheduling of airport runway operations using stochastic branch and bound methods. Transport Res Part C Emerg Technol 45:119–137

20. Samà M, D'Ariano A, Pacciarelli D (2013) Rolling horizon approach for aircraft scheduling in the terminal control area of busy airports. Proc Soc Behav Sci 80:531–552
21. Beasley JE, Sonander J, Havelock P (2001) Scheduling aircraft landings at London Heathrow using a population heuristic. J Oper Res Soc 52(5):483–493
22. Pohl M, Artigues C, Kolisch R (2022) Solving the time-discrete winter runway scheduling problem: a column generation and constraint programming approach. Eur J Oper Res 299(2):674–689
23. Cecen RK, Cetek C, Kaya O (2020) Aircraft sequencing and scheduling in TMAs under wind direction uncertainties. Aeronaut J 124(1282):1896–1912
24. Prakash R, Desai J, Piplani R (2022) An optimal data-splitting algorithm for aircraft sequencing on a single runway. Ann Oper Res 309(2):587–610
25. Ahmadian MM, Salehipour A (2022) Heuristics for flights arrival scheduling at airports. Int Trans Oper Res 29(4):2316–2345
26. Sáez R, Polishchuk T, Schmidt C, Hardell H, Smetanová L, Polishchuk V, Prats X (2021) Automated sequencing and merging with dynamic aircraft arrival routes and speed management for continuous descent operations. Transport Res Part C Emerg Technol 132:103402
27. Ng KKH, Lee CKM, Chan FT, Qin Y (2017) Robust aircraft sequencing and scheduling problem with arrival/departure delay using the min-max regret approach. Transport Res Part E Logist Transport Rev 106:115–136
28. Rodríguez-Díaz A, Adenso-Díaz B, González-Torre PL (2017) Minimizing deviation from scheduled times in a single mixed-operation runway. Comput Oper Res 78:193–202
29. Kaplan Z, Çetek C (2020) Yapay Bağişiklik Metasezgiseli İle Tek Pistli Havaalanlarinda İniş Siralamasinin Eniyilenmesi. Eskişehir Osmangazi Üniversitesi Mühendislik ve Mimarlık Fakültesi Dergisi 28(3):321–331
30. Rodríguez-Díaz A, Adenso-Díaz B, González-Torre PL (2019) Improving aircraft approach operations taking into account noise and fuel consumption. J Air Transp Manag 77:46–56
31. Hammouri AI, Braik MS, Al-Betar MA, Awadallah MA (2020) ISA: a hybridization between iterated local search and simulated annealing for multiple-runway aircraft landing problem. Neural Comput Appl 32(15):11745–11765
32. Faye A (2018) A quadratic time algorithm for computing the optimal landing times of a fixed sequence of planes. Eur J Oper Res 270(3):1148–1157
33. Dahlberg J, Granberg TA, Polishchuk T, Schmidt C, Sedov L (2018) Capacity-driven automatic design of dynamic aircraft arrival routes. In: AIAA/IEEE digital avionics systems conference—proceedings, September
34. Pawelek A, Lichota P, Dalmau R, Prats X (2017) Arrival traffic synchronisation with required time of arrivals for fuel-efficient trajectories. In: Proceedings of the 17th ATIO-AIAA aviation technology, integration, and operations conference
35. Dalmau R, Alenka J, Prats X (2017) Combining the assignment of predefined routes and RTAs to sequence and merge arrival traffic. In: 17th AIAA aviation technology, integration, and operations conference
36. Sáez R, Dalmau R, Prats X (2018) Optimal assignment of 4D close-loop instructions to enable CDOs in dense TMAs. In: AIAA/IEEE digital avionics systems conference—proceedings, September
37. Sáez R, Prats X, Polishchuk T, Polishchuk V (2020) Traffic synchronization in terminal airspace to enable continuous descent operations in trombone sequencing and merging procedures : an implementation study for Frankfurt airport. Transp Res Part C 121:102875
38. Liang M, Delahaye D, Sbihi M, Ma J (2016) Multi-layer point merge system for dynamically controlling arrivals on parallel runways. In: 2016 IEEE/AIAA 35th digital avionics systems conference, September
39. Cecen RK (2022) Fuel-optimal aircraft arrival operations in extended terminal maneuvering areas. Transportation Research Record, 03611981221074362
40. Sáez GR, Prats X (2020) Comparison of fuel consumption of continuous descent operations with required times of arrival. In: ICRAT
41. BADA (2013) User manual for the base of aircraft data (BADA) Revision 3.11. BADA, Bretigny-sur-Orge, Fransa
42. Kaplan Z, Cetek C (2019) An approach sequencing model for minimum total fuel consumption and most efficient use of runway capacity, Master Thesis, Eskisehir Technical University